Pressure sensitivity of ANME-3 predominant anaerobic methane oxidizing community from coastal marine Lake Grevelingen sediment

C. Cassarini[a,b*], Y. Zhang[c] and P. N. Lens[a,b]

[a]UNESCO-IHE, Institute for Water Education, P.O.Box 3015, 2601 DA , Delft, The Netherlands

[b] National University of Ireland Galway, University Road, Galway H91 TK33, Ireland

[c]State Key Laboratory of Microbial Metabolism, School of Life Sciences and Biotechnology, Shanghai Jiao Tong University, Shanghai, People's Republic of China

*Corresponding author

Chiara Cassarini

National University of Ireland Galway

University Road, Galway H91 TK33, Ireland

Phone: +31(0)152151715

e-mail: chiara.cassarini@gmail.com

Abstract

Anaerobic oxidation of methane (AOM) coupled to sulfate reduction is mediated by, respectively, anaerobic methanotrophic archaea (ANME) and sulfate reducing bacteria (SRB). When a microbial community from coastal marine Lake Grevelingen sediment, containing ANME-3 as the most abundant type of ANME, was incubated under a pressure gradient (0.1- 40 MPa) for 77 days, ANME-3 was more pressure sensitive than the SRB. ANME-3 activity was higher at lower (0.1, 0.45 MPa) over higher (10, 20 and 40 MPa) CH_4 total pressures. Moreover, the sulfur metabolism was shifted upon changing the incubation pressure: only at 0.1 MPa elemental sulfur was detected in a considerable amount and SRB of the *Desulfobacterales* order were more enriched at elevated pressures than the *Desulfubulbaceae*. This study provides evidence that ANME-3 can be constrained at shallow environments, despite the scarce bioavailable energy, because of its pressure sensitivity. Besides, the association between ANME-3 and SRB can be steered by changing solely the incubation pressure.

Importance

Anaerobic oxidation of methane (AOM) coupled to sulfate reduction is a biological process largely occurring in marine sediments, which contributes to the removal of almost 90% of sedimentary methane, thereby controlling methane emission to the atmosphere. AOM is mediated by slow growing archaea, anaerobic methanotrophs (ANME) and sulfate reducing bacteria. The enrichment of these microorganisms has been challenging, especially considering the low solubility of methane at ambient temperature and pressure. Previous studies showed strong positive correlations between the growth of ANME and the methane pressure, since the higher the pressure the more methane is dissolved. In this research, a shallow marine sediment

was incubated under methane pressure gradients. The investigated effect of pressure on the AOM-SR activity, the formation sulfur intermediates and the microbial community structure is important to understand the pressure influence on the processes and the activity of the microorganisms involved to further understand their metabolism and physiology.

Introduction

Anaerobic oxidation of methane (AOM) coupled to sulfate reduction (SR) is a major sink in the oceanic methane (CH_4) budget. The net stoichiometry of this reaction is shown in Eq. 1 (1):

$$CH_4 + SO_4^{2-} \rightarrow HCO_3^- + HS^- + H_2O \qquad \Delta G^{\circ\prime} = -16.6 \text{ kJ mol}^{-1} \text{ } CH_4 \qquad \text{(Eq. 1)}$$

The thermodynamics of this reaction depend on the concentration of dissolved CH_4. CH_4 is poorly soluble: 1.3 mM is its concentration in sea water at ambient pressure and at 15°C (2). Theoretically, an elevated CH_4 pressure favors the AOM coupled to SR (AOM-SR) bioconversion since i) the Gibbs free energy becomes more negative at higher CH_4 partial pressures and ii) the dissolved CH_4 concentration increases and is thus more bioavailable (Table 1). Thus, the activity and the growth of the microorganisms mediating the process, namely anaerobic methanotrophs (ANME) and sulfate reducing bacteria (SRB), is expected to be higher at elevated pressures.

ANME are grouped into three distinct clades, i.e. ANME-1, ANME-2 and ANME-3 based on the phylogenetic analysis of their 16S rRNA genes (3-5). *In vitro* incubations of ANME-1 and ANME-2 dominated microbial communities from deep sea sediments in high-pressure reactors showed indeed a strong positive relation of the activity of the microorganisms capable of the AOM-SR process with the CH_4 partial pressure, up to 12 MPa (6-10). In the ANME-2 dominated

shallow marine sediment of Eckernförde Bay, the AOM-SR rate increased linearly with the CH_4 pressure from 0.00 to 0.15 MPa when incubated in batch, determining an affinity constant (K_m) for CH_4 at least higher than 0.075 MPa (1.1 mM) (11). The K_m for CH_4 of ANME-2 present in Gulf of Cadiz sediment is about 37 mM (9), which is equivalent to 3 MPa CH_4 partial pressure. This ANME-2 dominated sediment has its optimum pressure at the in situ pressure (S. Bhattarai, Y. Zhang, and P.N.L Lens, submitted for publication). In contrast, the CH_4 partial pressure influenced the growth of different subtypes of ANME-2 and SRB (i.e. at 10.1 MPa only the ANME-2c and SEEP-SRB2 subtypes were enriched) from the Eckernförde Bay marine sediment incubated for 240 days in a high-pressure membrane capsule bioreactor (12).

Studying the effect of pressure on ANME and SRB will thus help understand the growth of the different ANME clades and their SRB partner. Finding ANME-SRB consortia that can grow fast at ambient pressure is of great importance for the application of AOM-SR in the desulfurization of industrial wastewater. Sulfate and other sulfur oxyanions, such as thiosulfate, sulfite or dithionite, are contaminants discharged in fresh water by industrial activities such as food processing, fermentation, coal mining, tannery and paper processing. Biological desulfurization under anaerobic conditions is a well-known biological treatment, in which these sulfur oxyanions are anaerobically reduced to sulfide (13-15). The produced sulfide precipitates with the metals, thus enabling their recovery (16). In the process of groundwater, mining or inorganic wastewater desulfurization, electron donor for sulfate reduction needs to be supplied externally. Electron donors such as ethanol, hydrogen, methanol, acetate, lactate and propionate (13) are usually supplied, but these increase the operational and investment costs (16). The use of easily accessible and low-priced electron donors such as CH_4 is therefore appealing for field-scale

84 applications (17). Moreover, from a logistic, economical and safety view point, bioreactors
85 operating at ambient conditions are preferred over those operated at high pressures.

86 Coastal marine sediment from Lake Grevelingen (the Netherlands) hosts both ANME and SRB
87 (18). Among the ANME types, ANME-3 is predominant, which makes this sediment a beneficial
88 inoculum to investigate the effects of pressure on ANME-3. ANME-3 is often found in cold seep
89 areas and mud volcanoes with high CH_4 partial pressures and relatively low temperatures (10,
90 19, 20). Therefore, the shallow marine sediment from Lake Grevelingen was incubated at
91 different pressures (0.1, 0.45, 10, 20, and 40 MPa) to study the influence of pressure on the
92 AOM-SR activity, but also on the methanogenic activity and the potential formation of carbon,
93 e.g. acetate or methanethiol, (21) and sulfur, e.g. elemental sulfur or polysulfides (22),
94 intermediates. Moreover, phylogenetic analysis and visualization of microorganisms by
95 fluorescence in-situ hybridization (FISH) were used to study the activity and the shifts in cell
96 morphology, community composition and aggregation upon incubation of marine Lake
97 Grevelingen sediment at different pressures in batch for 77 days.

98 ## Results

99 *Conversion rates of sulfur compounds*

100 The highest sulfide production rates of the coastal marine Lake Grevelingen sediment was in the
101 incubations at the *in situ* pressure (0.45 MPa) and 10 MPa: 270 and 258 µmol g_{VSS}^{-1} d^{-1},
102 respectively (Figure 1a). The sulfide production rate at 40 MPa was 109 µmol g_{VSS}^{-1} d^{-1},
103 comparable to the rate with no CH_4 in the headspace, 99 µmol g_{VSS}^{-1} d^{-1} (Figure 1a). Similarly,
104 high SR rates were recorded for the incubations at 0.45 MPa and 10 MPa (Figure 1b): 297 and

278 µmol g_{VSS}^{-1} d^{-1}, respectively. In contrast, the SR rate at 0.1 MPa was 257 µmol g_{VSS}^{-1} d^{-1}, while the sulfide production was only 157 µmol g_{VSS}^{-1} d^{-1} (Figures 1b and 1a).

Sulfide was produced in almost all the incubations (Figure 2), with the exception of the incubation without biomass (Figure 2g). The sulfate concentration profiles varied with initial incubation pressure: at 0.45 MPa sulfate was reduced to sulfide in a 1:1 ratio (Figure 2b), whereas sulfate was not reduced anymore after 40 days of incubation at 40 MPa (Figure 2e). At 0.45 MPa, 0.98 mmol of sulfate was consumed and exactly 0.98 mmol of total dissolved sulfide was produced, closing the sulfur balance. In the incubation at 0.1 MPa, 0.37 mmol of elemental sulfur was produced along with 0.54 mmol of sulfide (Figure 2a). In the other incubations at different pressures, hardly any elemental sulfur was formed (Figures 2c-2g). Instead, long chain polysulfides were formed along the incubation depending on the pressure (Figure 3), but in small amounts (≤ 2 µmol per vessel): 2 µmol S_6^{2-} per vessel was determined at 0.45 MPa CH_4 pressure (Figure 3b) and 1.2 and 1.4 µmol S_6^{2-} per vessel at 10 MPa and 20 MPa, respectively (Figures 3c and 3d).

AOM rates

The AOM rates were calculated from the DIC produced from $^{13}CH_4$, from which the K_m for CH_4 of the marine Lake Grevelingen sediment was determined to be around 1.7 mM. The DIC production rates followed a similar trend as the sulfide production rates: the highest rate was found at 0.45 MPa and the lowest rate at 40 MPa: 320 and 38 µmol g_{VSS}^{-1} d^{-1}, respectively (Figure 1c). In the incubation at 0.45 MPa (*in situ* pressure), the total DIC produced from CH_4 was similar to the sulfide produced: ~0.9 mmol per vessel (Supporting information, Figure S1b and Figure 2b). However, sulfide was produced from the start for all the incubations, while the

total DIC from CH_4 was mainly produced only after 40 days of incubation (Figure 2 and Supporting information, Figure S1). Similar trends were found for all the other incubations at different pressure, except for the vessel without CH_4, where only sulfide production (0.3 mmol/ vessel) was recorded.

Methanogenesis

CH_4 was produced in all the incubations, with the exception of the batches without biomass (Supporting information, Figure S2). The highest amount of CH_4 formed was recorded in the vessel at 0.1 MPa (Supporting Information, Figure S2b). The highest methanogenic rate was determined in the control vessel without CH_4 (N_2 in the headspace) and at 0.1 MPa: 44 and 31 µmol g_{VSS}^{-1} d^{-1}, respectively, while it was below 5 µmol g_{VSS}^{-1} d^{-1} in all the other batch incubations (Supporting information, Figure S2a). Assuming that all the total ^{12}C-DIC was produced from the oxidation of other carbon sources than CH_4, its production rate was low in almost all the incubations: lower than 3 µmol g_{VSS}^{-1} d^{-1}, except for the incubation without CH_4 (64 µmol g_{VSS}^{-1} d^{-1}, data not shown).

Community shifts as a function of incubation pressure: total cell numbers

The total bacterial and archaeal cellular numbers were accessed from Q-PCR data performed on samples after 77 days of incubation (Figure 4). The highest increase in active cells, from 6 to 8×10^7 cells ml^{-1}, was found in the incubation at the *in situ* pressure of 0.45 MPa. In the incubation at 40 MPa, the amount of active total bacteria and archaea cells decreased from 6.5 to 5.8×10^7 cells ml^{-1} (Figure 4a). Based on Q-PCR results, archaea grew in all the incubations, while copy numbers of bacteria decreased in the incubation without CH_4 and at 20 MPa. The total number of archaea increased the most in the incubation at 20 MPa (Figure 4b).

Based on the 16s rRNA gene analysis, both archaeal and bacterial communities had shifted along the 77 days incubation (Figure 5). The most abundant OTUs (operational taxonomic unit) with archaeal signature are shown in Figure 5a. Specifically, the abundance of ANME-3 among all the archaea increased the most in incubations at 0.45 and 0.1 MPa, i.e. respectively three and two times more than at the start of the incubation (Figure 5a). ANME-2a/b reads increased the most at 20 MPa: 27 times more than at the start of the incubation (Figure 5a). Sequences of methanogens, specifically belonging to the *Methanomicrobiales*, were more abundant after the incubation at 0.1 MPa, rather than at higher partial pressures, where *Thaumarchaeota* and *Woesearchaeaota* were more abundant in incubations at 10, 20 and even 40 MPa (Figure 5a).

The bacterial communities were very diverse in all the incubations, the ones with the highest percentage are shown in Figure 5b. The absolute abundance of the *Desulfobulbaceae* (DBB) as calculated from their 16s rRNA gene according to Q-PCR and Miseq results increased or remained similar at the lower pressure incubations (0.1 and 0.45 MPa), but the percentage of DBB in the total bacterial community decreased at more elevated pressures (10, 20 and 40 MPa). Differently, the absolute abundance of *Desulfobacteraceae*, as DSS, increased in all the incubations at different pressures, with the highest percentage of reads retrieved in the incubation at 20 MPa (Figure 5b). The percentage of OTUs as assigned to *Desulfovibrio*, *Desulfuromonas*, *Halomonas* and *Sulfurovum* genes decreased in all the batch incubations (Figure 5b).

Community shifts as a function of incubation pressure: FISH analysis

ANME-3 and DBB were visualized in all the batch incubations (Figures 6a-6c). At the start of the incubation (t = 0 days), ANME-3 cells were preferentially visualized in aggregates with other cells (data not shown). FISH images after 77 days of incubation showed variations in the

aggregate morphology depending on the incubation pressure (Figure 6). At 0.1 and 0.45 MPa, ANME-3 was more abundant than at the start, while the DBB cells were not found concomitant to the ANME-3 cells (Figure 6a) and, even if present, the ANME-3 cells outnumbered the DBB cells (Figure 6b). In the 10 MPa incubation, ANME-3 was visualized more scattered and not in clusters as at the lower pressures, whereas DBB cells were even more rarely pictured (Data not shown). At 20 MPa, ANME-3 and DBB cells were rare, however, the stained cells formed tight ANME-3/DBB aggregates (Figure 6c). At 40 MPa, ANME-3 and DBB were the least abundant and scattered and no aggregates could be found (data not shown).

Differently than ANME-3, more ANME-2 cells were visualized in the 77 days incubations at higher (10, 20 and 40 MPa) than at lower (0.1 and 0.45 MPa) incubation pressures (Figures 6d-6f). DSS, the most common SRB bacterial partner of ANME-2, were most abundant at 0.1 MPa. At lower pressure they were mainly visualized together with ANME-2 (Figure 6d). At 20 MPa only clusters of ANME-2 cells were visualized without DSS (Figure 6e).

Discussion

Pressure effect on AOM in marine Lake Grevelingen sediment

This study showed that AOM and SR processes in Lake Grevelingen sediment depend on the CH_4 total pressure. According to Eq. 1, the reaction rate is expected to be stimulated by the elevated CH_4 partial pressure when the other parameters remain the same (Table 1). This expectation has been commonly accepted and has been shown in communities dominated by ANME-1, i.e. hydrocarbon seep in the Monterey canyon sediment (23) and ANME-2, i.e. Eckernförde Bay (24, 25) and Gulf of Cadiz sediment (S. Bhattarai, Y. Zhang, and P.N.L. Lens, submitted for publication). In contrast, the AOM-SR process by the ANME-3 dominated marine

193 Lake Grevelingen sediment has an optimal pressure at 0.45 MPa among all tested conditions
194 (Figure 1). This is in accordance with their natural habitat, i.e. the *in situ* pressure of marine Lake
195 Grevelingen is 0.45 MPa, but contrasts the theoretical thermodynamic calculation (Table 1), that
196 predicts a higher CH_4 solubility and thus a higher activity based on reported *Km* values, i.e. 37
197 mM as calculated from an ANME-2 predominant enrichment originated from the Gulf of Cadiz
198 (9). The calculated K_m value on CH_4 based on our ANME-3 dominated inoculum is much lower
199 than previously reported: around 1.7 mM. Thus, the ANME cells from Grevelingen marine
200 sediment have a higher affinity for CH_4 than the ANME-2 from the Gulf of Cadiz, explaining
201 why a higher pressure, i.e. higher dissolved CH_4 concentration, did not result in a higher AOM
202 rate (Figu 1c). As a matter of fact, higher pressure resulted in a lower number of ANME-3 cells
203 and ANME-3 proliferated only at lower pressures incubation (0.1 and 0.45 MPa). This indicates
204 ANME-3 cells of marine Lake Grevelingen are non-piezophilic, which are easily damaged upon
205 pressure elevation and require extra energy to cope with the damage (26). ANME-3 are found in
206 cold seep areas and mud volcanoes with high CH_4 partial pressures (~10 MPa) and relatively low
207 temperatures (10, 19, 20). However, Lake Grevelingen is a shallow sediment with high
208 abundance of ANME-3 (18) and likely contains different subtypes than the ones found in deep
209 sea sediments, which cannot cope with a high pressure.

210 *Pressure effect on ANME types*

211 The ANME-3 type is usually visualized in association with DBB as sulfate reducing partner (10,
212 19). FISH analysis showed that the DBB cells were not as high in number as the ANME-3 cells
213 in any of the incubations (Figures 6a-6c), but they increased the most at the 0.1 MPa incubation
214 (data not shown). In a recent study describing the microbial ecology of Lake Grevelingen
215 sediment (incubation pressure = 0.1 MPa), the two species (ANME-3 and DBB) could not be

visualized together and the DBB cells were much less abundant than ANME-3 (18), similarly to this study (Figure 6a). At 0.1 and 0.45 MPa, ANME-3 cells were visualized in aggregates mainly detached from DBB cells (Figures 6a and 6b). ANME-3 cells have been visualized without bacterial partner before (20, 27), suggesting that this ANME type is supporting a metabolism independent of an obligatory bacterial association. In contrast, as ANME-3 and DBB decreased in number at higher pressures, most of the ANME-3 and DBB visualized at 20 MPa were forming small ANME-3/DBB clusters, suggesting that they have mutual benefits at this pressure (Figure 6c).

Sequences of ANME-2 were also found by Miseq analysis (Figure 5a) and visualized by FISH (Figures 6d-6f) in all incubations. ANME-2a/b cells were higher in number in the incubation at higher pressures (10 and 20 MPa). Also many DSS were found in all the batch incubations and, as for ANME-2, they were more abundant at higher pressures (10 and 20 MPa). ANME-2 and DSS were mainly visualized in aggregates (Figure 6d), especially at lower pressures (0.1 and 0.45 MPa). The cooperative interaction between the ANME-2 and DSS is still under debate: Milucka et al. (22) stated that a synthrophic partner might not be required for ANME-2 and that they can be decoupled by using external electron acceptors (28), whereas recent studies have shown direct electron transfer between the two (ANME-2 and DSS) partners (29, 30). Besides, the DSS might have proliferated by growth on organic carbon compounds released by damaged or killed piezosensitive microorganisms.

Effect of pressure on sulfur cycle in marine Lake Grevelingen sediment

Figures 2 and 3 shows that the total pressure steers the sulfur cycling in the marine Lake Grevelingen sediment community. At 0.1 MPa CH_4 pressure, the reduced sulfate was converted

238 to both sulfide and zero-valent sulfur (Figure 2a). At 0.45 MPa (the incubation with the highest
239 AOM-SR activity), the sulfur balance was closed by solely the sulfide production (Figure 2b).
240 The production of elemental sulfur was repressed at elevated CH_4 pressures (Figure 2b-2e).
241 Elemental sulfur has been considered as intermediate in the AOM-SR process, which is
242 consumed by ANME to generate energy (22). Milucka et al. (22) showed that ANME-2 cells
243 could stand along without the metabolic support of the bacterial partner, assuming that CH_4 was
244 oxidized to bicarbonate and sulfate was reduced to disulfide (S_2^{2-}) through zero-valent sulfur as
245 an intracellular intermediate. The amount of disulfide or other polysulfides formed during the
246 incubations (Figure 3) was very low, in most cases below the detection limit (0.1 µmol). The
247 formation of these intermediate sulfur compounds in the ANME process needs to be further
248 elucidated using e.g. isotopic labeled sulfate (^{35}S) and nanometre scale secondary ion mass
249 spectrometry (NanoSIMS) analysis.

250 A shift from sulfate reducers (e.g. *Desulfobacterales*) to sulfur reducers (e.g.
251 *Desulforomonadales*) was observed in the bacterial community from low to high CH_4 partial
252 pressure (Figure 5b). Sulfur reducing bacteria, e.g. *Desulfovibrio* or *Desulforomonas*, are more
253 abundant at high CH_4 partial pressure (10, 20, 40 MPa), whereas sulfate reducing DBB are more
254 abundant in the incubations at lower CH_4 total pressure (Figure 5b), where they were present in
255 ANME-DBB aggregates and had the highest AOM-SR rates (Figure 1).

256 *In vitro demonstration of SR-AOM supported ecosystem in Lake Grevelingen*

257 This study showed that CH_4 and sulfate were an effective energy source supporting SR-AOM in
258 the microbial ecosystem from the marine Lake Grevelingen sediment (Figure 1). Apparent *in*
259 *vitro* biomass growth was observed, especially at 0.45 MPa which is the *in situ* pressure, with

CH_4 and sulfate supplied as the sole energy sources (Figure 1). At incubation conditions similar to *in situ* conditions (p = 0.45 MPa, T = 15ºC, pH = 7), the AOM and SR rates reached approximately 0.3 mmol g_{VSS}^{-1} d^{-1}. These rates are comparable or even higher than the *in vitro* AOM rates of ANME-1 or ANME-2 dominated biomass, e.g. the rate obtained after the enrichment of Eckernförde Bay sediment dominated by ANME-2 type cells for more than 800 days in a continuous membrane bioreactor (31). Moreover, the AOM-SR rate measured in this study at 0.45 MPa is even higher than the AOM rate coupled to denitrification, which is thermodynamically much more favorable ($\Delta G^{0'}$ = -924 kJ mol^{-1} CH_4) (32) than AOM-SR ($\Delta G^{0'}$ = -16.6 kJ mol^{-1} CH_4, Eq. 1).

It should be noted that even after two months incubation, the abundance of the responsible microorganisms, i.e. all detected types of ANME and SRB cells, is quite low: 17.8 $\times 10^5$ and 11.4 $\times 10^5$ number of copies per mL of wet sediment of ANME-3 and ANME-2, respectively, in the total community (data not shown). The ANME-3 cells present in the marine Lake Grevelingen possess high specific AOM-SR rates and thus, can be of great potential to be applied in the industry after enrichment. The SR rate with CH_4 as electron donor should be around 100 mmol g_{VSS}^{-1} d^{-1} to be competitive with the SR rates achieved with other electron donors, such as hydrogen or ethanol (31, 33), which is still much higher than what was obtained in this study.

Methanogenic activity in marine Lake Grevelingen sediment was previously described by Egger et al. (34) and confirmed in this study at low pressure (0.1 MPa) or when no CH_4 was added in the incubation (Supporting Information, Figure S2). At 0.1 MPa, the CH_4 production rate was 31 µmol g_{VSS}^{-1} d^{-1} and the AOM rate was 186 µmol g_{VSS}^{-1} d^{-1}. Trace CH_4 oxidation occurs during methanogenesis and the archaea involved compete with SRB for acetate (12, 24). Thus, the

282 determined AOM at 0.1 MPa cannot account for the net AOM-SR, as it is partly due to the
283 methanogenic activity.

284 At high pressures (0.45, 10 MPa), AOM-SR was preferred (Figure 1) over methanogenesis
285 (Supporting Information, Figure S2). Methanogenesis becomes less thermodynamically
286 favorable at high pressures, less free energy (12 kJ mol^{-1} less) is released upon changing the
287 incubation pressure from 0.1 to 10 MPa (24). Timmers et al. (12) found that at 10 MPa net
288 AOM-SR occurred, while at 0.1 MPa methanogenesis and trace CH_4 oxidation dominated. In this
289 study, the optimal AOM-SR was 0.45 MPa: the SR activity decreased at pressures higher than 10
290 MPa, while AOM activity already decreased at pressures higher than 0.45 MPa (Figures 1b and
291 1c).

292 ## Conclusions

293 This is the first study showing that the active ANME from the shallow marine Lake Grevelingen
294 sediment preferred lower (0.1 and 0.1 MPa) over elevated (10, 20, 40 MPa) pressures, in contrast
295 to previous studies that show strong positive correlations between the growth of ANME-1/2 and
296 the CH_4 pressure. Pressure steered the abundance and structure of the different types of ANME
297 and SRB. The ANME-3 type was predominantly enriched in incubations at low pressures,
298 whereas high pressures enhanced ANME-2 proliferation. Similarly, a shift from sulfate reducers
299 to sulfur reducers was observed in the bacterial community from low (0.1 and 0.45 MPa) to high
300 (10, 20, 40 MPa) CH_4 partial pressure. This research highlights that ANME-3 from marine Lake
301 Grevelingen can be enriched at rather low CH_4 partial pressures, which is important to further
302 understand their metabolism and physiology.

303 ## Materials and Methods

Site description and sampling procedure

The sediment was obtained from the Scharendijke Basin in the marine Lake Grevelingen (water depth of 45; position 51° 44.541' N; 3° 50.969' E), which is a former estuary in the southwestern part of the Netherlands. The sampling site characteristics, biochemical processes and the microbial community composition have been described previously (18, 34-36). Coring was done in November 2013 on the vessel R/V Luctor by the Royal Netherlands Institute for Sea Research (Yerseke, the Netherlands). The sampling procedure has been described in Bhattarai et al. (18), the sediment was kept at 4 ºC in the dark in serum bottles with a headspace of CH_4 until use.

Experimental design

The effect of the pressure on the CH_4 oxidation, SR and CH_4 production rate of the marine Lake Grevelingen sediment was assessed with 0.07 (± 0.01) g volatile suspended solids (g_{VSS}) in 200 ml pressure vessels incubated in triplicates at 0.1 MPa, 0.45 MPa (mimicking the in situ conditions), 10 MPa, 20 MPa and 40 MPa. The vessels were flushed and pressurized with 100 % CH_4, from which about 20% was ^{13}C-labeled CH_4 ($^{13}CH_4$). The marine Lake Grevelingen sediment used as inoculum was incubated with artificial saline mineral medium with sulfate (10 mM) at 15°C for 77 days. Two different control incubations were prepared in triplicates at 0.45 MPa: without biomass and without CH_4, but with nitrogen in the headspace.

Slurry samples were taken every week for chemical analysis. Approximately 1 mL sample was taken by attaching a connector and a vacuum tube to the exit port while gently opening the tap. Weight and pressure were measured in the vacuum tube before and after sampling. Pressure in each vessel was restored by adding fresh basal medium using a high performance liquid chromatography (HPLC) pump (SSI, USA).

Chemical analysis

The gas composition was measured on a gas chromatograph-mass spectrometer (GC-MS Agilent 7890A-5975C). The GC-MS system was composed of a Trace GC equipped with a GC-GasPro column (30 m by 0.32 mm; J & W Scientific, Folsom, CA) and an Ion-Trap MS. Helium was the carrier gas at a flow rate of 1.7 ml min^{-1}. The column temperature was 30ºC. The fractions of CH_4 and CO_2 in the headspace were derived from the peak areas in the gas chromatograph, while the fractions of $^{13}CH_4$, $^{12}CH_4$, $^{12}CO_2$ and $^{13}CO_2$ were derived from the mass spectrum as done by (37).

Total dissolved sulfide was measured by using the methylene blue method (Hach Lange method 8131) and a DR5000 Spectrophotometer (Hach Lange GMBH, Düsseldorf, Germany). Samples for sulfate and thiosulfate analysis were first diluted in a solution of zinc acetate (5 g/L) and centrifuged at 13,200g for 3 min to remove insoluble zinc sulfide, and filtrated through 0.45 µm membrane filters. Sulfate and thiosulfate concentrations were then determined by ion chromatography (Metrohm 732 IC Detector) with a METROSEP A SUPP 5 - 250 column. The pH was checked by means of pH paper.

Polysulfides were methylated using the protocol by Kamyshny et al. (38) and analyzed by reversed-phase HPLC. Elemental sulfur from the slurry sample was extracted using methanol following the method described by Kamyshny et al. (39), but modified for small volumes. Dimethylpolysulfanes and extracted elemental sulfur were analyzed by an HPLC (HPLC 1200 Series, Agilent Technologies, USA) with diode array and multiple wavelength detector. A mixture of 90% MeOH and 10% water was used as eluent. A reversed phase C-18 column (Hypersil ODS, 125 × 4.0 mm, 5 µm, Agilent Technologies, USA) was used for separation.

Concentrations of dimethylpolysulfanes from Me_2S_3 to Me_2S_7 were calculated from calibration curves of polysulfides standards prepared following the protocol of Milucka et al. (22). UV detector response to Me_2S_8 was calculated by the algorithm discussed in Kamyshny et al. (40).

The VSS was estimated at the beginning of the experiment on the basis of the difference between the dry weight total suspended solids and the ash weight of the sediment according to the procedure outlined in Standard Method (41).

Rate calculations

Both AOM and SR rates were expressed as µmol of sulfide or dissolved inorganic carbon (DIC) production per gram of VSS per day (µmol g_{VSS}^{-1} d^{-1}). For the AOM rate calculation, the total production of ^{13}C-carbonate species (^{13}C-DIC), i.e. $^{13}CO_2$ in both liquid and gas phases, $H^{13}CO_3^-$ and $^{13}CO_3^{2-}$ in liquid phase, were first calculated. Considering that only 20% of CH_4 was $^{13}CH_4$, the total ^{13}C-DIC was divided by the fractional abundance of ^{13}C in the CH_4 measured and used for each batch to determine the total amount of DIC produced from CH_4 oxidation (42). For methanogenesis and for the formation of carbonate species from other carbon sources than CH_4, $^{12}CH_4$ and $H^{12}CO_3^-$ were taken respectively, and divided by the ^{12}C fractional abundance. A line was plotted over the period where the decrease or increase of the different compounds ($^{12}CH_4$, $^{13}CH_4$, $H^{12}CO_3^-$, $H^{13}CO_3^-$, total dissolved sulfide and sulfate) was linear (at least four consecutive points) to estimate the rates (24), which were divided by the biomass content in the vessels (0.07 ± 0.01 g_{VSS} in each vessel).

DNA extraction

DNA was extracted by using a FastDNA® SPIN Kit for soil (MP Biomedicals, Solon, OH, USA) by following the manufacturer's protocol. Approximately 0.5 g of the sediment was used for

DNA extraction from the initial inoculum and ~0.5 ml of liquid obtained by washing the polyurethane foam packing with nuclease free water was used for extracting DNA from the enriched slurry. The extracted DNA was quantified and quality was checked as described by Bhattarai et al. (18).

PCR amplification for 16S rRNA genes and Illumina Miseq data processing

The DNA was amplified using bar coded archaea specific primer pair Arc516F and reverse Arc855R. The PCR reaction mixture was prepared as described by Bhattarai et al. (18), however, the PCR amplification was performed using a touch-down temperature program. PCR conditions consisted of a pre-denaturation step of 5 min at 95^{o}C, followed by 10 touch-down cycles of 95^{o}C for 30 sec, annealing at 68^{o}C for 30 sec with a decrement per cycle to reach the optimized annealing temperature of 63^{o}C and extension at 72^{o}C. This was followed by 25 cycles of denaturation at 95^{o}C for 30 sec and 30 sec of annealing and extension at 72^{o}C. The final elongation step was extended for 10 min.

The primer pairs used for bacteria were forward bac520F 5'-3' AYT GGG YDT AAA GNG and reverse Bac802R 5'-3' TAC NNG GGT ATC TAA TCC (43). The following program was used: initial denaturation step at 94^{o}C for 5 min, followed by denaturation at 94^{o}C for 40 sec, annealing at 42 ^{o}C for 55 sec and elongation at 72^{o}C for 40 sec (30 cycles). The final elongation step was extended to 10 min. 5 µl of the amplicons were visualized by standard agarose gel electrophoresis (1% agarose gel, a running voltage of 120 V for 30 min, stained by gel red) and documented using a UV transilluminator with Gel Doc XR System (Bio-Rad, USA).

After checking the correct band size, 150 µl of PCR amplicons were loaded in 1% agarose gel and electrophoresis was performed for 120 min at 120 V. The gel bands were excited under UV

light and the PCR amplicons were cleaned using E.Z.N.A.® Gel Extraction Kit by following the manufacturer's protocol (Omega Biotek, USA). The purified DNA amplicons were sequenced by an Illumina HiSeq 2000 (Illumina, San Diego, USA) and analyzed according to the procedure described in Bhattarai et al. (18). A total of 40,000 (± 20,000) sequences were assigned to archaea and bacteria examining the tags assigned to the amplicons. More detailed analytical procedure has been described by Bhattarai et al. (18). These sequence data have been submitted to the NCBI GenBank database under BioProject accession number PRJNA415004 (direct link: http://www.ncbi.nlm.nih.gov/bioproject/415004).

Quantitative real-time PCR (Q-PCR)

Archaeal and bacterial clones were used to prepare Q-PCR standard. Plasmids were isolated using the Plasmid Kit (Omega Biotek, USA). The plasmid was digested with the EcoR I enzyme. After digestion purification was done by gel extraction (Gel extraction Kit, Omega Biotek, USA). The copy number was calculated from the total mass and the nucleic acid concentration. Extracted DNA from the sediment at the start and at the end of the incubation period (11 weeks) was used for qPCR analysis to quantify archaea and bacteria. Amplifications were done in triplicates in a 7500 Real-Time PCR System (Applied Biosystem). Each reaction (20µl) contained 1× Power SYBR-Green PCR MasterMix (Applied Biosystems), 0.4µM of each primer, and 5 ng template DNA. The 16S rRNA genes of bacterial origin were amplified using the primers Bac331f (5'-TCCTACGGGAGGCAGCAGT3') and Bac797r (5'-GGACTACCAGGGTCTAATCCTGTT-3') (44). Cycling conditions were 95°C for 10 min; and 40 cycles at 95°C for 30 sec and 60°C for 30 sec and 72°C for 30 sec. Archaea were quantified using the primer set Arch349f (5′-GYGCASCAGKCGMGAAW-3′) and Arch806r (5′-GGACTACVSGGGTATCTAAT-3') (45). Cycling conditions were 95°C for 10 min; and 40

cycles at 95°C for 30 sec and 50°C for 30 sec and 72°C for 30 sec. Triplicate standard curves were obtained with 10-fold serial dilutions ranged between 10^7 and 10^{-2} copies per µl of plasmids. The efficiency of the reactions was up to 100% and the R^2 of the standard curves were up to 0.999.

Cell visualization and counting by FISH

At the start and at the end of the incubation period (11 weeks), 200 µL of sample from each vessel was fixed in a final 2% paraformaldehyde solution for 4 h on ice. The samples were washed twice with 1x phosphate buffer saline solution (PBS). Then, it was stored in a mixture of PBS and ethanol (EtOH), with a PBS/EtOH ratio of 1:1 at -20^{o}C as previously described by (3). This sample was used for cell counting and FISH analysis.

100 µL of stored sample was diluted with nuclease free water, sonicated for 40 sec and then filtered on 0.2 µm membrane filters. For cell counting, 200-300 µL of 20x SYBR green solution (Takara, Japan) was added on top of the filter and incubated in the dark at room temperature for 30min. The filters were dried and mounted on a glass slide with 100 µL glycerol 10%. For FISH analysis, the filtrated sample was hybridized with the archaeal probe ARCH915 (46), the bacterial probe EUB I-III (47), with different CY3-labeled ANME probes: ANME-1 350 (3), ANME-2 538 (48), ANME-3 1249 (10) and the Cy5-labelled SRB specific probes for *Desulfosarcina / Desulfococcus* (DSS) DSS658 (3) and *Desulfobulbus* (DBB) DBB660 (49). Cells were counterstained with 4', 6-diamidino-2-phenylindole (DAPI) (50). The hybridization of the samples and microscopic visualization of the hybridized cells were performed as described previously (51).

Acknowledgements

We acknowledge Filip Meysman from the Royal Netherlands Institute of Sea Research (NIOZ, Yerseke, The Netherlands) for providing the Lake Grevelingen sediment. The authors are grateful for using the analytical facilities of the Centre for Chemical Microscopy (ProVIS) at the Helmholtz-Centre for Environmental Research which is supported by European regional Development Funds (EFRE and Europe funds Saxony) and the Helmholtz Association. The authors acknowledge Dr. Niculina Musat (team leader of ProVIS) for her advice and practical support during FISH analysis. This research was funded by the Erasmus Mundus Joint Doctorate Programme ETeCoS^3 (Environmental Technologies for Contaminated Solids, Soils and Sediments) under the grant agreement FPA no. 2010-0009 and the National Natural Science Foundation of China (grant number: 41476123).

References

1. Reeburgh WS. 2007. Oceanic methane biogeochemistry. Chem Rev 107:486-513.
2. Yamamoto S, Alcauskas JB, Crozier TE. 1976. Solubility of methane in distilled water and seawater. J Chem Eng Data 21:78-80.
3. Boetius A, Ravenschlag K, Schubert CJ, Rickert D, Widdel F, Gieseke A, Amann R, Jørgensen BB, Witte U, Pfannkuche O. 2000. A marine microbial consortium apparently mediating anaerobic oxidation of methane. Nature 407:623-626.
4. Hinrichs KU, Hayes JM, Sylva SP, Brewer PG, DeLong EF. 1999. Methane-consuming archaebacteria in marine sediments. Nature 398:802-805.
5. Knittel K, Lo T, Boetius A, Kort R, Amann R, Lösekann T. 2005. Diversity and distribution of methanotrophic archaea at cold seeps. Appl Environ Microbiol 71:467-479.

6. Deusner C, Meyer V, Ferdelman TG. 2009. High-pressure systems for gas-phase free continuous incubation of enriched marine microbial communities performing anaerobic oxidation of methane. Biotechnol Bioeng 105:524-533.

7. Krüger M, Treude T, Wolters H, Nauhaus K, Boetius A. 2005. Microbial methane turnover in different marine habitats. Palaeogeogr Palaeoecl 227:6-17.

8. Nauhaus K, Boetius A, Krüger M, Widdel F. 2002. In vitro demonstration of anaerobic oxidation of methane coupled to sulphate reduction in sediment from a marine gas hydrate area. Environ Microbiol 4:296-305.

9. Zhang Y, Henriet JP, Bursens J, Boon N. 2010. Stimulation of in vitro anaerobic oxidation of methane rate in a continuous high-pressure bioreactor. Biores Technol 101:3132-3138.

10. Niemann H, Lösekann T, de Beer D, Elvert M, Nadalig T, Knittel K, Amann R, Sauter EJ, Schlüter M, Klages M, Foucher JP, Boetius A. 2006. Novel microbial communities of the Haakon Mosby mud volcano and their role as a methane sink. Nature 443:854-858.

11. Meulepas RJW, Jagersma CG, Khadem AF, Buisman CJN, Stams AJM, Lens PNL. 2009. Effect of environmental conditions on sulfate reduction with methane as electron donor by an Eckemförde Bay enrichment. Environ Sci Technol 43:6553-6559.

12. Timmers PH, Gieteling J, Widjaja-Greefkes HA, Plugge CM, Stams AJM, Lens PNL, Meulepas RJ. 2015. Growth of anaerobic methane-oxidizing archaea and sulfate-reducing bacteria in a high-pressure membrane capsule bioreactor. Appl Environ Microbiol 81:1286-1296.

13. Liamleam W, Annachhatre AP. 2007. Electron donors for biological sulfate reduction. Biotechnol Adv 25:452-463.

14. Sievert SM, Kiene RP, Schulz-Vogt HN. 2007. The sulfur cycle. Oceanography 20:117-123.

15. Weijma J, Veeken A, Dijkman H, Huisman J, Lens PNL. 2006. Heavy metal removal with biogenic sulphide: advancing to full-scale., p 321-333. *In* Cervantes F, Pavlostathis S, van Haandel A (ed), Advanced biological treatment processes for industrial wastewaters, principles and applications. IWA publishing, London.

16. Meulepas RJW, Stams AJM, Lens PNL. 2010. Biotechnological aspects of sulfate reduction with methane as electron donor. Rev Environ Sci Biotechnol 9:59-78.

17. Gonzalez-Gil G, Meulepas RJW, Lens PNL. 2011. Biotechnological aspects of the use of methane as electron donor for sulfate teduction, p 419-434. *In* Murray M-Y (ed), Comprehensive biotechnology, 2nd ed, vol 6. Elsevier B.V., Amsterdam, the Netherlands.

18. Bhattarai S, Cassarini C, Gonzalez-Gil G, Egger M, Slomp CP, Zhang Y, Esposito G, Lens PNL. 2017. Anaerobic methane-oxidizing microbial community in a coastal marine sediment: anaerobic methanotrophy dominated by ANME-3. Microb Ecol 74:608-622.

19. Lösekann T, Knittel K, Nadalig T, Fuchs B, Niemann H, Boetius A, Amann R. 2007. Diversity and abundance of aerobic and anaerobic methane oxidizers at the Haakon Mosby Mud Volcano, Barents Sea. Appl Environ Microbiol 73:3348-3362.

20. Vigneron A, Cruaud P, Pignet P, Caprais J-C, Cambon-Bonavita M-A, Godfroy A, Toffin L. 2013. Archaeal and anaerobic methane oxidizer communities in the Sonora Margin cold seeps, Guaymas Basin (Gulf of California). ISME J 7:1595-1608.

21. Valentine DL, Reeburgh WS, Hall R. 2000. New perspectives on anaerobic methane oxidation. Environ Microbiol 2:477-484.

505 22. Milucka J, Ferdelman TG, Polerecky L, Franzke D, Wegener G, Schmid M, Lieberwirth
506 I, Wagner M, Widdel F, Kuypers MMM. 2012. Zero-valent sulphur is a key intermediate
507 in marine methane oxidation. Nature 491:541-546.
508 23. Girguis PR, Cozen AE, De Long EF. 2005. Growth and population dynamics of
509 anaerobic methane-oxidizing archaea and sulfate-reducing bacteria in a continuous-flow
510 bioreactor. Appl Environ Microbiol 71:3725-3733.
511 24. Meulepas RJW, Jagersma CG, Zhang Y, Petrillo M, Cai H, Buisman CJN, Stams AJM,
512 Lens PNL. 2010. Trace methane oxidation and the methane dependency of sulfate
513 reduction in anaerobic granular sludge. FEMS Microbiol Ecol 72:261-271.
514 25. Timmers PHA, Suarez-Zuluaga DA, van Rossem M, Diender M, Stams AJM, Plugge
515 CM. 2015. Anaerobic oxidation of methane associated with sulfate reduction in a natural
516 freshwater gas source. ISME J 10:1400-1412.
517 26. Zhang Y, Li X, Bartlett DH, Xiao X. 2015. Current developments in marine
518 microbiology: high-pressure biotechnology and the genetic engineering of piezophiles.
519 Curr Opin Microbiol 33:157-164.
520 27. Omoregie EO, Mastalerz V, de Lange G, Straub KL, Kappler A, Røy H, Stadnitskaia A,
521 Foucher J-P, Boetius A. 2008. Biogeochemistry and community composition of iron- and
522 sulfur-precipitating microbial mats at the Chefren mud volcano (Nile Deep Sea Fan,
523 Eastern Mediterranean). Appl Environ Microbiol 74:3198-3215.
524 28. Scheller S, Yu H, Chadwick GL, McGlynn SE, Orphan VJ. 2016. Artificial electron
525 acceptors decouple archaeal methane oxidation from sulfate reduction. Science 351:703-
526 707.

527 29. McGlynn SE, Chadwick GL, Kempes CP, Orphan VJ. 2015. Single cell activity reveals
528 direct electron transfer in methanotrophic consortia. Nature 526:531-535.
529 30. Wegener G, Krukenberg V, Ruff SE, Kellermann MY, Knittel K. 2016. Metabolic
530 capabilities of microorganisms involved in and associated with the anaerobic oxidation of
531 methane. Front Microbiol 7:46.
532 31. Meulepas RJW, Jagersma CG, Gieteling J, Buisman CJN, Stams AJM, Lens PNL. 2009.
533 Enrichment of anaerobic methanotrophs in sulfate-reducing membrane bioreactors.
534 Biotechnol Bioeng 104:458-470.
535 32. Deutzmann JS, Schink B. 2011. Anaerobic oxidation of methane in sediments of Lake
536 Constance, an oligotrophic freshwater lake. Appl Environ Microbiol 77:4429-4436.
537 33. Suarez-Zuluaga DA, Timmers PHA, Plugge CM, Stams AJM, Buisman CJN, Weijma J.
538 2016. Thiosulphate conversion in a methane and acetate fed membrane bioreactor.
539 Environ Sci Pollut 23:2467-2478.
540 34. Egger M, Lenstra W, Jong D, Meysman FJR, Sapart CJ, van der Veen C, Röckmann T,
541 Gonzalez S, Slomp CP. 2016. Rapid sediment accumulation results in high methane
542 effluxes from coastal sediments. PloS ONE 11:e0161609.
543 35. Hagens M, Slomp CP, Meysman FJR, Seitaj D, Harlay J, Borges AV, Middelburg JJ.
544 2015. Biogeochemical processes and buffering capacity concurrently affect acidification
545 in a seasonally hypoxic coastal marine basin. Biogeosciences 12:1561-1583.
546 36. Sulu-Gambari F, Seitaj D, Meysman FJR, Schauer R, Polerecky L, Slomp CP. 2016.
547 Cable bacteria control iron–phosphorus dynamics in sediments of a coastal hypoxic
548 basin. Environ Sci Technol 50:1227-1233.

549 37. Shigematsu T, Tang Y, Kobayashi T, Kawaguchi H, Morimura S, Kida K. 2004. Effect
550 of dilution rate on metabolic pathway shift between aceticlastic and nonaceticlastic
551 methanogenesis in chemostat cultivation. Appl Environ Microbiol 70:4048-4052.
552 38. Kamyshny A, Ekeltchik I, Gun J, Lev O. 2006. Method for the determination of
553 inorganic polysulfide distribution in aquatic systems. Anal Chem 78:2631-2639.
554 39. Kamyshny A, Borkenstein CG, Ferdelman TG. 2009. Protocol for quantitative detection
555 of elemental sulfur and polysulfide zero-valent sulfur distribution in natural aquatic
556 samples. Geostand Geoanal Res 33:415-435.
557 40. Kamyshny A, Goifman A, Gun J, Rizkov D, Lev O. 2004. Equilibrium distribution of
558 polysulfide ions in aqueous solutions at 25 °C: a new approach for the study of
559 polysulfides' equilibria. Environ Sci Technol 38:6633-6644.
560 41. APHA. 1995. Standard methods for the examination of water and wastewater,
561 Washington DC, USA.
562 42. Zhang Y, Maignien L, Stadnitskaia A, Boeckx P, Xiao X, Boon N. 2014. Stratified
563 community responses to methane and sulfate supplies in mud volcano deposits: insights
564 from an in vitro experiment. PLoS ONE 9:e113004.
565 43. Song Z-Q, Wang F-P, Zhi X-Y, Chen J-Q, Zhou E-M, Liang F, Xiao X, Tang S-K, Jiang
566 H-C, Zhang CL, Dong H, Li W-J. 2013. Bacterial and archaeal diversities in Yunnan and
567 Tibetan hot springs, China. Environ Microbiol 15:1160-1175.
568 44. Nadkarni MA, Martin FE, Jacques NA, Hunter N. 2002. Determination of bacterial load
569 by real-time PCR using a broad-range (universal) probe and primers set. Microbiology
570 148:257-266.

571 45. Takai K, Horikoshi K. 2000. Rapid detection and quantification of members of the
572 archaeal community by quantitative PCR using fluorogenic probes. Appl Environ
573 Microbiol 66:5066-5072.
574 46. Stahl DA. 1991. Development and application of nucleic acid probes, p 205-248. *In*
575 Stackebrandt E, Goodfellow M (ed), Nucleic acid techniques in bacterial systematics.
576 John Wiley & Sons, Chichester, UK.
577 47. Daims H, Brühl A, Amann R, Schleifer K-H, Wagner M. 1999. The domain-specific
578 probe EUB338 is insufficient for the detection of all bacteria: development and
579 evaluation of a more comprehensive probe set. Syst Appl Microbiol 22:434-444.
580 48. Treude T, Knittel K, Blumenberg M, Seifert R, Boetius A. 2005. Subsurface microbial
581 methanotrophic mats in the Black Sea Appl Environ Microbiol 71:6375-6378.
582 49. Daly K, Sharp RJ, McCarthy AJ. 2000. Development of oligonucleotide probes and PCR
583 primers for detecting phylogenetic subgroups of sulfate-reducing bacteria. Microbiology
584 146:1693-1705.
585 50. Wagner M, Amann R, Lemmer H, Schleifer KH. 1993. Probing activated sludge with
586 oligonucleotides specific for proteobacteria: inadequacy of culture-dependent methods
587 for describing microbial community structure Appl Environ Microbiol 59:1520-1525.
588 51. Snaidr J, Amann R, Huber I, Ludwig W, Schleifer KH. 1997. Phylogenetic analysis and
589 in situ identification of bacteria in activated sludge. Appl Environ Microbiol 63:2884-
590 2896.
591 52. Duan Z, Mao S. 2006. A thermodynamic model for calculating methane solubility,
592 density and gas phase composition of methane-bearing aqueous fluids from 273 to 523K
593 and from 1 to 2000bar. Geochim Cosmochim Ac 70:3369-3386.

Tables

595 **Table 1.** Gibbs free energy of AOM coupled to SR ($\Delta_r G'$) at different CH_4 total pressures and
596 assuming the following *in vitro* conditions: temperature 15°C, pH 7.0, HCO_3^- 30 mM, SO_4^{2-} 10
597 mM and HS^- 0.01 mM. The maximum dissolved CH_4 concentration at a salinity of 32‰ and
598 15°C at different CH_4 partial pressure was determined by the Duan model (52). AOM and SR
599 rates determined in this (marine Lake Grevelingen sediment) and other studies. [a] = data from
600 Timmers et al. (12): AOM-SR rate of Eckernförde sediment based on ^{13}C- carbonate species
601 production and [b] = data from Zhang et al. (9): AOM-SR activity of Capt Aryutinov Mud Volcano
602 sediment based on sulfide production.

Pressure (MPa)	**Concentration (mM)**	**$\Delta_r G'$ (KJ mol^{-1})**	**AOM rate (µmol g_{vss}^{-1} day^{-1})**	**SR rate (µmol g_{vss}^{-1} day^{-1})**	**AOM-SR rate (µmol g_{vss}^{-1} day^{-1})**
			This study		**Other studies**
0.1	1.4	-25.8 kJ mol^{-1} CH_4	186.4	257.4	5.8[a]
0.2	2.9	-27.5 kJ mol^{-1} CH_4	-		0.18[b]
0.45	6.4	-29.4 kJ mol^{-1} CH_4	324.0	297	-
1	14.0	-31.3 kJ mol^{-1} CH_4	-		3.46[b]
4.5	55.6	-34.6 kJ mol^{-1} CH_4	-		8.64[b]
8	87.3	-35.7 kJ mol^{-1} CH_4	-		9.22[b]
10	101.9	-36.1 kJ mol^{-1} CH_4	109.5	277.6	20.9[a]
20	149.8	-37.0 kJ mol^{-1} CH_4	91.7	162.4	-
40	198	-37.7 kJ mol^{-1} CH_4	38.5	154.3	-

603

Figure legends

Figure 1. (a) Sulfide production rate, (b) SR rate and AOM rate for incubations at different pressure and controls without CH_4, but with N_2 in the headspace and without biomass. Error bars indicate the standard deviation (n=3).

Figure 2. Concentration profiles of total dissolved sulfide (◆), sulfate (■) and elemental sulfur (▲) for the incubation at (a) 0.1MPa, (b) 0.45 MPa, (c) 10 MPa, (d) 20 MPa, (e) 40 MPa, (f) without CH_4, and (g) without biomass. Error bars indicate the standard deviation (n=3).

Figure 3. Total dissolved sulfide (◆) and polysulfides concentration, namely S_2^{2-} (●), S_3^{2-} (✱), S_4^{2-} (✕), S_5^{2-} (■). S_6^{2-} (▲), during the incubation of Grevelingen sediment at (a) 0.45 MPa, (b) 0.1MPa, (c) 10 MPa, (d) 20 MPa, and (e) 40 MPa. Error bars indicate the standard deviation (n=3).

Figure 4. (a) Total number of active cells and (b) number of copies of archaea and bacteria from Q-PCR analysis per ml of wet sediment in each pressurized vessel at the start (t=0 days) and at the end of the incubation (t=77 days). Error bars indicate the standard deviation (n=3).

Figure 5. Heat map of top most abundant 16s rRNA sequences at the beginning (t=0) and at the end of the incubations (t=77 days) of the marine Lake Grevelingen sediment at different CH_4 pressures and control without CH_4 in the headspace showing the phylogenetic affiliation up to family level as derived by high throughput sequencing of (a) archaea and (b) bacteria.

Figure 6. FISH images (a-c) from CY3-labeled ANME-3 in red color, CY5-labeled *Desulfobulbus* (DBB) in green after 77 days of incubation at (a) 0.1 MPa, (b) 0.45 MPa and (c) 20 MPa total CH_4 pressure. FISH images (d-f) from CY3-labeled ANME-2 in red color, CY5-

625 labeled *Desulforsarcina/Desulfococcus* group (DSS) in green after 77 days of incubation at (a)
626 0.45 MPa, (b) 20 MPa and (c) 40 MPa total CH_4 pressure. White scale bar representing 10 µm.

627 **Supplemental Material Legends**

628 **Figure S1**. (a) CH_4 production rates were calculated from the linear regression over at least four
629 successive measurements in which the calculated $^{12}CH_4$ increase over time was linear. (b) The
630 CH_4 produced was calculated from the $^{12}CH_4$. Methanogenic activity and CH_4 produced during
631 AOM were determined for incubations at different pressures and controls without CH_4, but with
632 N_2 in the headspace and without biomass. Error bars indicate the standard deviation (n=4).

633 **Figure S2**. Concentration profiles of methane oxidized ($^{13}CH_4$,) and dissolved inorganic
634 carbon (DIC,) calculated from the produced $^{13}CO_2$) during the incubation of marine Lake
635 Grevelingen sediment at (a) 0.1 MPa, (b) 0.45 MPa, (c) 10 MPa, (d) 20 MPa and (e) 40 MPa.

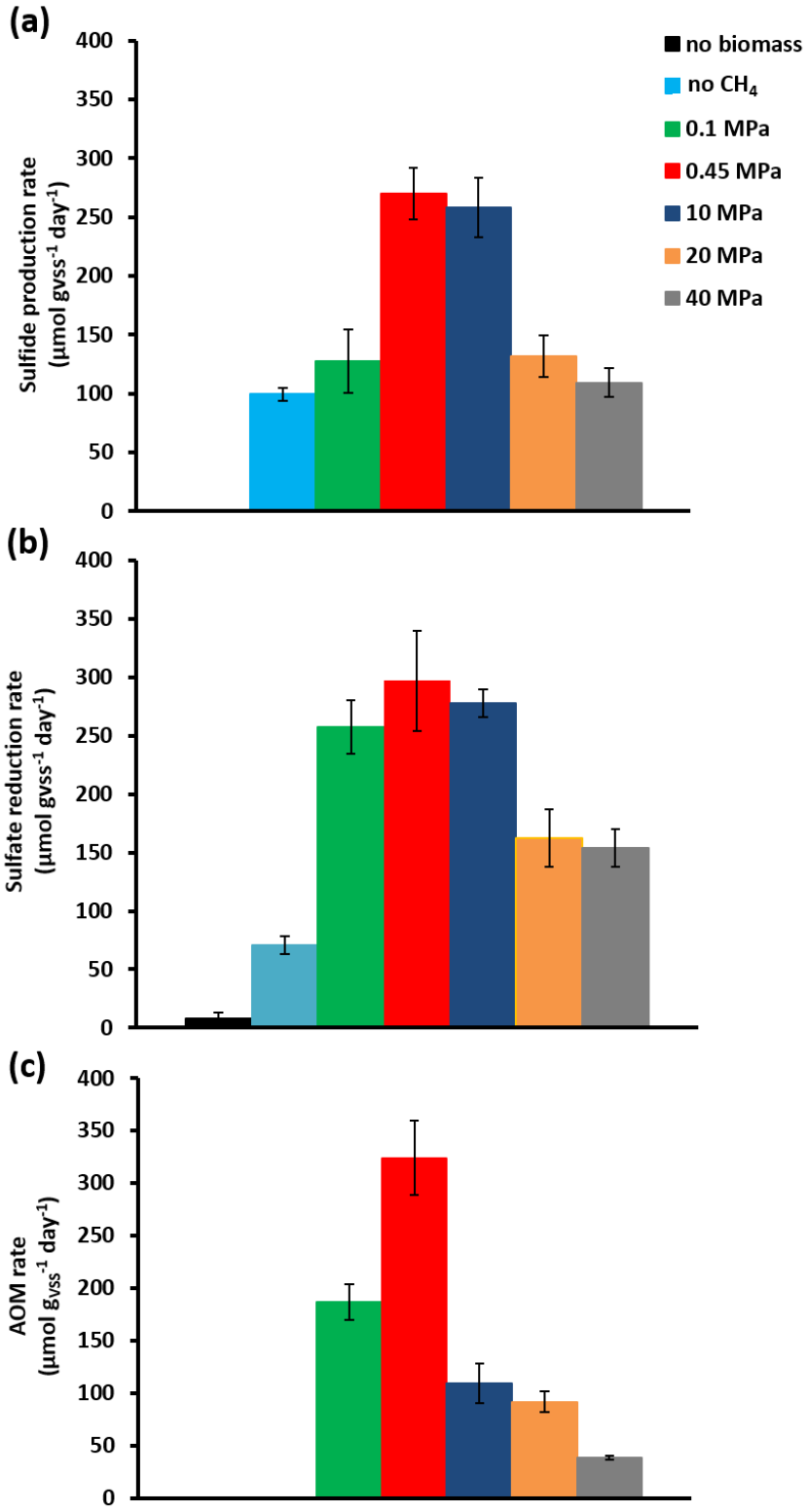

Figure 1. (a) Sulfide production rate, (b) SR rate and AOM rate for incubations at different pressure and controls without CH_4, but with N_2 in the headspace and without biomass. Error bars indicate the standard deviation (n=3).

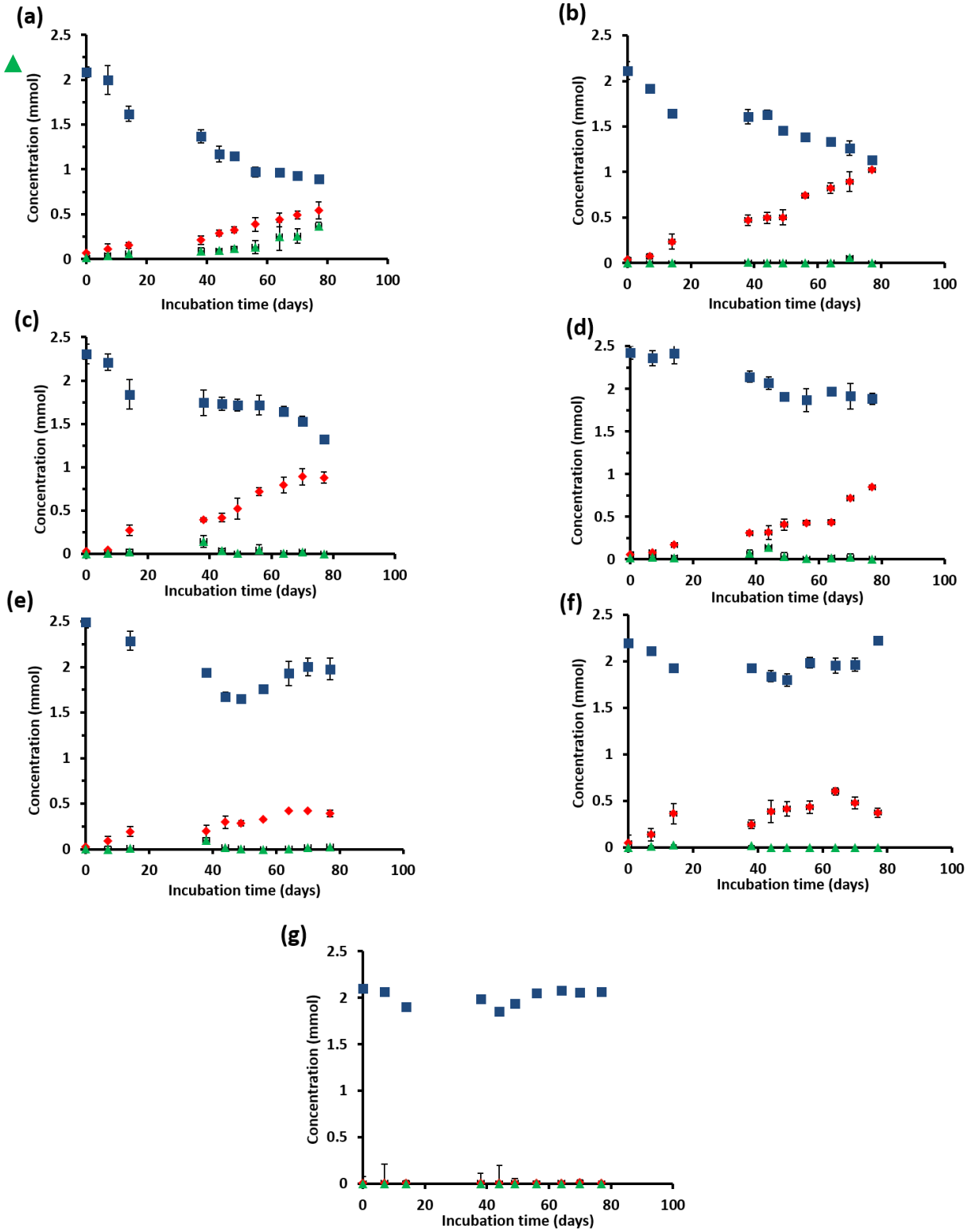

Figure 2. Concentration profiles of total dissolved sulfide (◆), sulfate (■) and elemental sulfur (▲) for the incubation at (a) 0.1MPa, (b) 0.45 MPa, (c) 10 MPa, (d) 20 MPa, (e) 40 MPa, (f) without CH_4, and (g) without biomass. Error bars indicate the standard deviation (n=3).

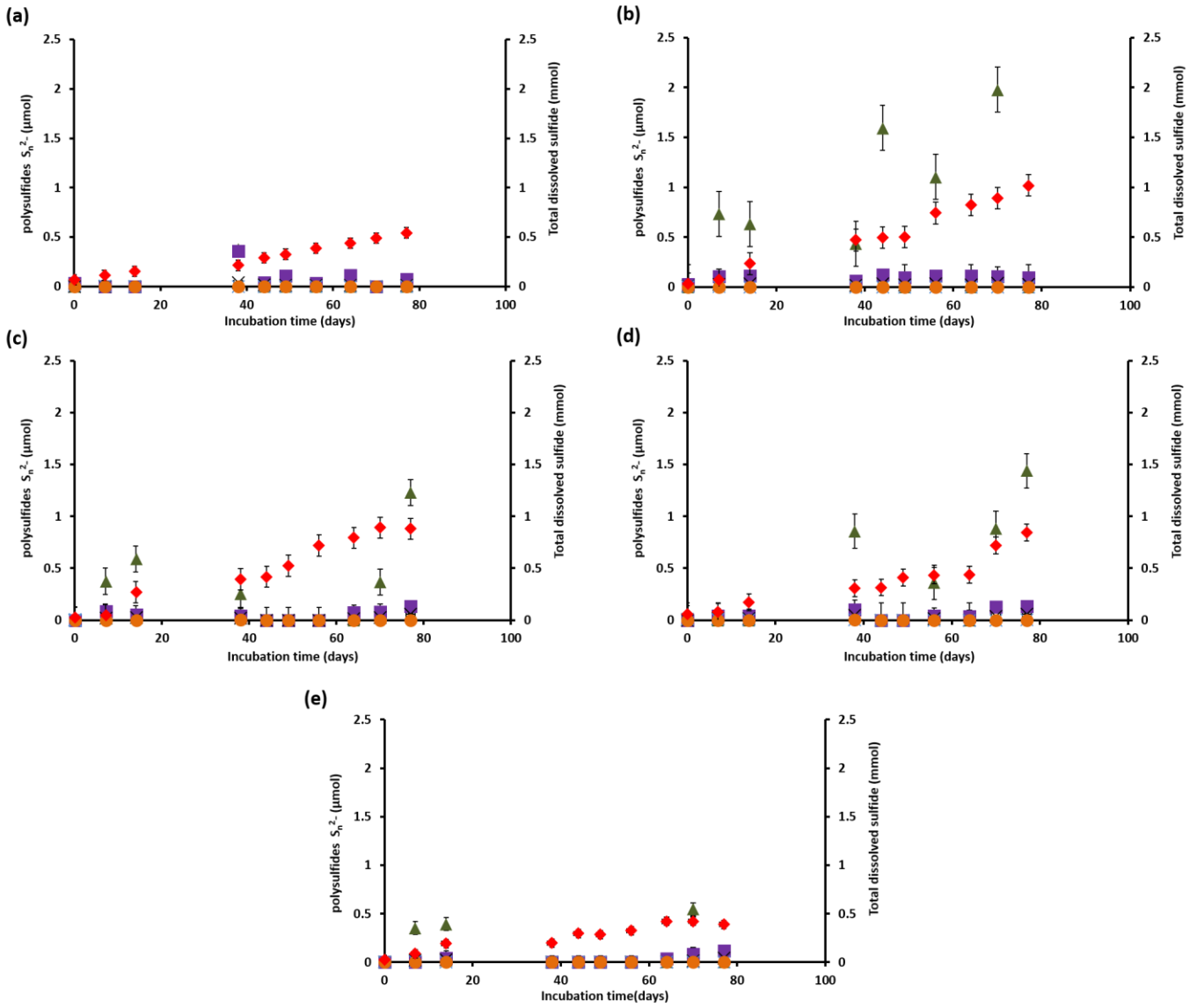

Figure 3. Total dissolved sulfide (◆) and polysulfides concentration, namely S_2^{2-} (●), S_3^{2-} (✳), S_4^{2-} (✕), S_5^{2-} (■). S_6^{2-} (▲), during the incubation of Grevelingen sediment at (a) 0.45 MPa, (b) 0.1MPa, (c) 10 MPa, (d) 20 MPa, and (e) 40 MPa. Error bars indicate the standard deviation (n=3).

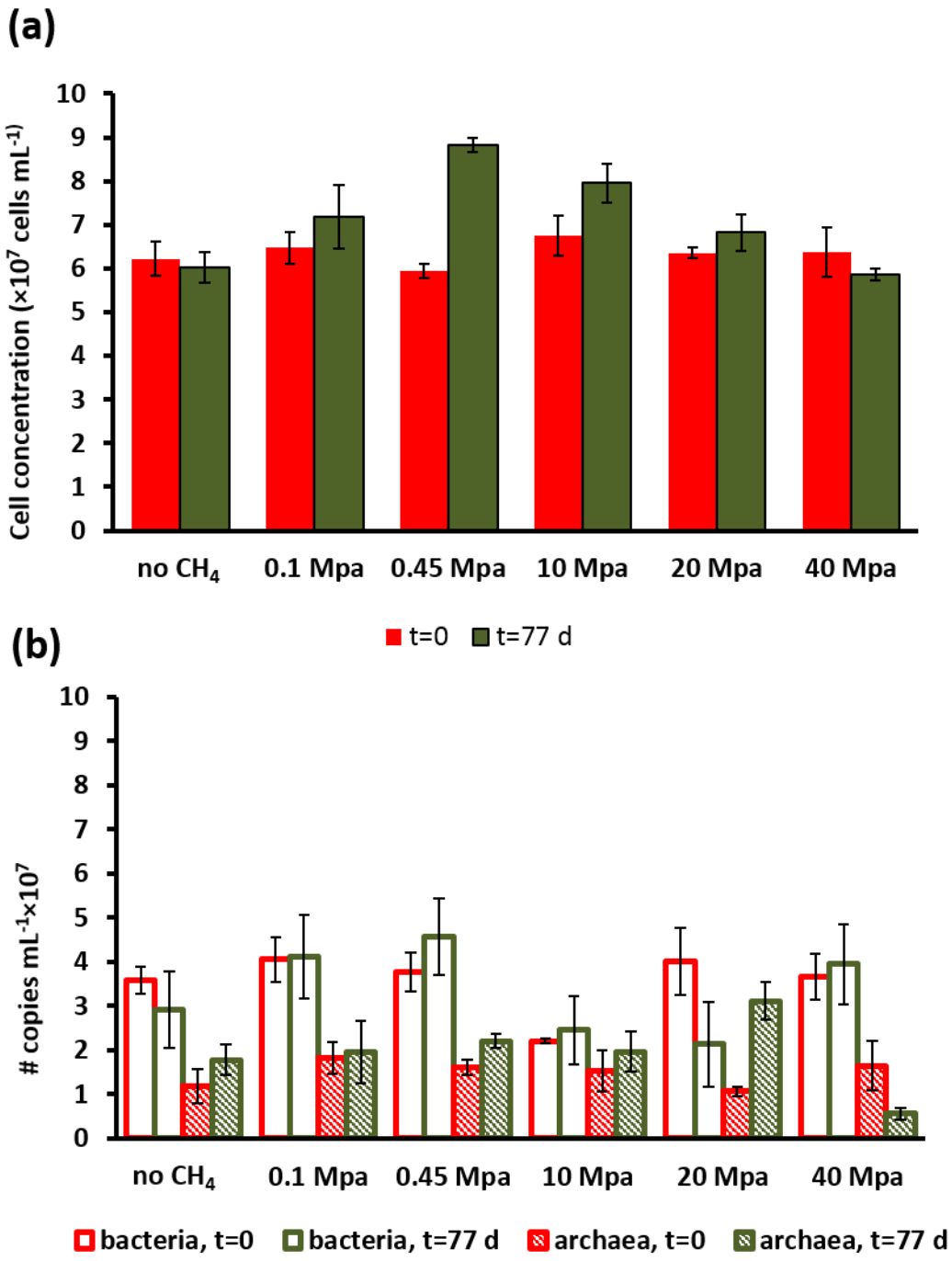

Figure 4. (a) Total number of active cells and (b) number of copies of archaea and bacteria from Q-PCR analysis per ml of wet sediment in each pressurized vessel at the start (t=0 days) and at the end of the incubation (t=77 days). Error bars indicate the standard deviation (n=3).

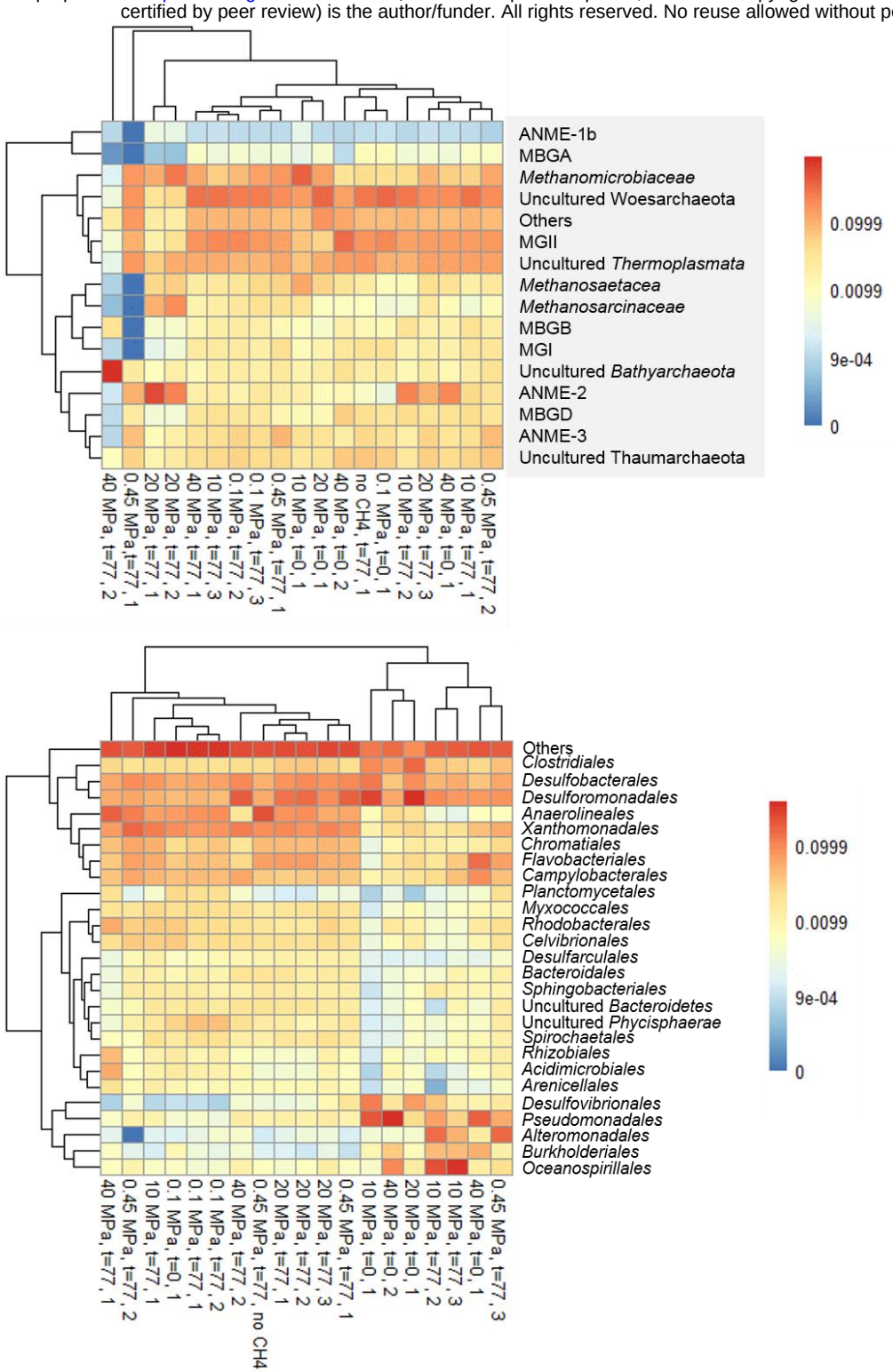

Figure 5. Heat map of top most abundant 16s rRNA sequences at the beginning (t=0) and at the end of the incubations (t=77 days) of the marine Lake Grevelingen sediment at different CH_4 pressures and control without CH_4 in the headspace showing the phylogenetic affiliation up to family level as derived by high throughput sequencing of (a) archaea and (b) bacteria.

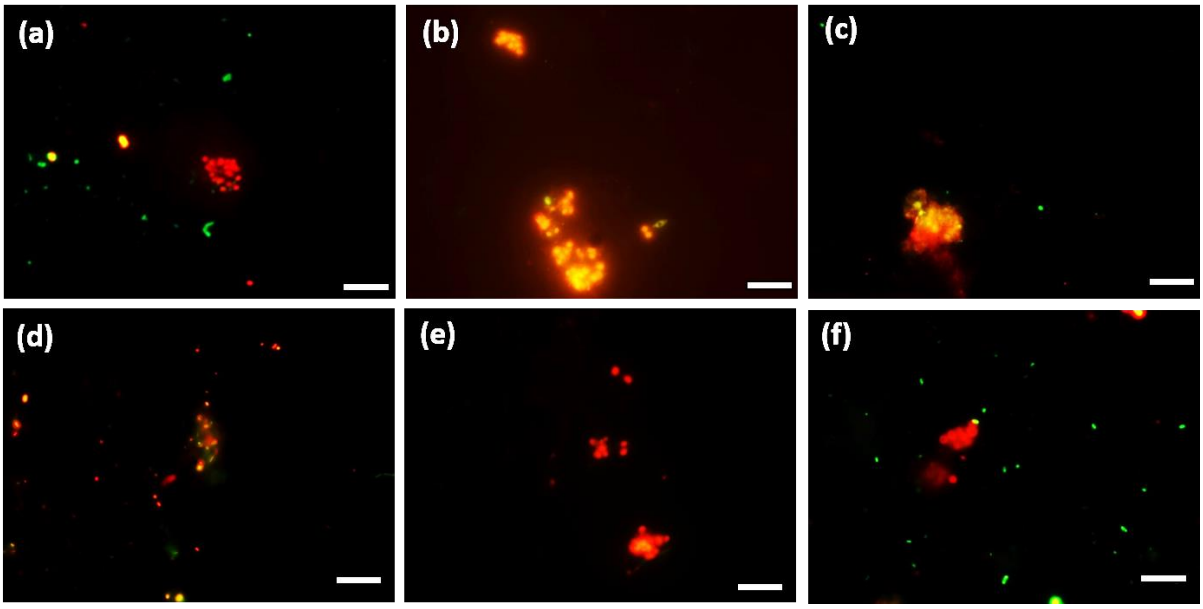

Figure 6. FISH images (a-c) from CY3-labeled ANME-3 in red color, CY5-labeled *Desulfobulbus* (DBB) in green after 77 days of incubation at (a) 0.1 MPa, (b) 0.45 MPa and (c) 20 MPa total CH_4 pressure. FISH images (d-f) from CY3-labeled ANME-2 in red color, CY5-labeled *Desulforsarcina/Desulfococcus* group (DSS) in green after 77 days of incubation at (a) 0.45 MPa, (b) 20 MPa and (c) 40 MPa total CH_4 pressure. White scale bar representing 10 µm.